ISBN: 978-3-95450-223-3 ISSN: 2673-7000 doi:10.18429/JACoW-NAPAC2019-WEPLH19

RECORD FAST CYCLING ACCELERATOR MAGNET BASED ON HIGH TEMPERATURE SUPERCONDUCTOR*

H. Piekarz†, S. Hays, J.N. Blowers, B. Claypool, V.D. Shiltsev, Fermilab, Batavia, IL, USA

Abstract

We report on the High Temperature Superconductor (HTS) based prototype accelerator magnet capable to operate at 12 *T/s B*-field ramping rate with a very low supporting cryogenic cooling power thus indicating a feasibility of its application in the accelerator requiring high repetition rate and high average beam power. The magnet is designed to simultaneously accelerate two particle beams in the separate beam gaps energized by a single conductor. The design, construction and the power test of the prototype fast-cycling HTS based accelerator magnet is presented while the more detailed description and power test data analysis s given in [1]. As example, the measured cryogenic power loss limit is discussed in terms of the feasibility of application of such a magnet for the construction of the 8 GeV dual proton beam Booster.

MOTIVATION

Next generation HEP facilities, such as muon colliders [2], future circular colliders [3, 4], high-intensity proton synchrotrons for neutrino research [5-7] accelerators demand substantially faster beam cycles which in turn require fast-cycling accelerator magnets with *dB/dt* of the order of tens to hundreds of *T/s*. As all these applications require accelerator magnets to operate in the rapid-cycling regime the fast-ramping magnetic field induces possibly very significant power losses in the power cable and in the magnetic core. The use of the superconducting cable instead of the normal conducting one to power accelerator magnets is expected to much reduce the *dB/dt* induced power loses in both magnetic core and cable and thus make accelerator construction more cost effective.

MAGNET DESIGN, CONSTRUCTION AND TEST ARRANGEMENT

The use of the superconductor versus normal conductor significantly reduces the cross-section of the power cable which in turn reduces the cross-section of the magnetic core. In this way the power losses induced by the fast-ramping magnetic field are minimized in both the cable and the magnetic core. In addition, the high current density of the superconductor allows the power cable to be arranged as a narrow slab which with the optimized position within the magnet core cable space allows for strong minimization of cable exposure to the core descending *B*-field. Magnet design with a slab-like conductor is shown in Fig. 1 where the *B*-field crossing cable space is less than 5% of the field in the beam gap. In addition, the HTS superconducting cable can operate within a very wide temperature margin. With the number of strands in the power cable allowing to carry the required transport current at the temperatures up to e.g. 35 K, the cable operational temperature of 4.5 K allows then for the 30 K temperature margin facilitating in this way operation of the quench detection and cable protection systems.

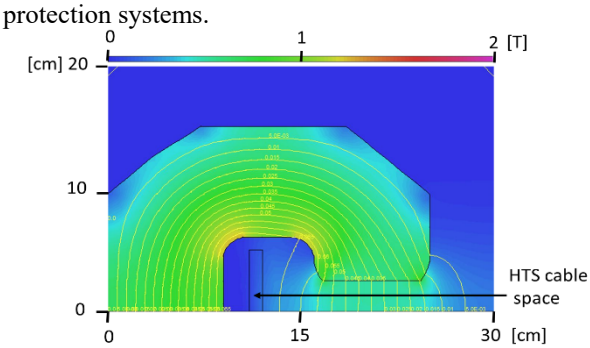

Figure 1: B-field simulation for 40 mm (vertical) x 100 mm (horizontal) gap of 1 T magnet.

For the HTS-based rapid-cycling accelerator magnet design we used the following criteria: (I) A single conductor coil energizes two magnet beam gaps allowing for the simultaneous acceleration of two beams while cutting in half the required accelerator ramping and operation power per beam, (II) The two beam gaps are aligned in the vertical plane allowing for the beam loss and/or beam particle decays to be emitted into the space away from the magnet and thus strongly suppressing potential for the radiation damage of the superconductor. The vertical alignment of the beam gaps also makes orbits of both beams equal and thus eliminating the orbit swapping required to equalize beams circulation periods for the acceleration in the common RF section. The conceptual view of the vertical dual-bore HTS accelerator magnet is shown in Fig. 2. The 0.5 m long test magnet with vertically arranged dual bean gaps of 10 mm (height) x 100 mm (width) and core of 620 mm x 255 mm cross-section is exactly of the shape as shown in Fig. 2. The 3-part core construction allows for simple assembly and installation of the HTS conductor coil. The full 3-turn conductor coil is shown in Fig. 3. The details of the HTS strands and copper tape windings are shown in Fig. 4. The 2 mm wide and 0.1 mm thick, HTS strands (Super-Power, Inc. [8]) are helically wound at 10 cm pitch on the surface of the helium conduit pipes made of 316LN stainless steel, 8 mm OD, 0.5 mm wall thickness. This arrangement makes ~ 1.05 mm averaged exposed width of a single HTS strand to the B-field. A single layer of the 0.1 mm thick, 12.5 mm wide oxygen-free high conductivity copper tape is wound helically over the strands to firmly secure their attachment to the cooling helium conduit pipe.

*Work supported by Fermi Research Alliance, LLC under contract No. DE-AC02-07CH1359 with the United States Department of Energy
†hpiekarz@fnal.gov

ISBN: 978-3-95450-223-3 ISSN: 2673-7000 doi:10.18429/JACoW-NAPAC2019-WEPLH19

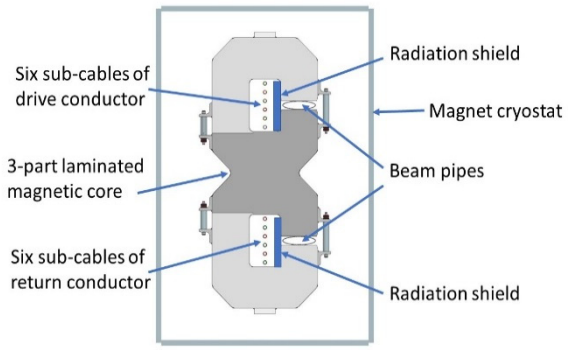

Figure 2: Conceptual design of HTS dual bore magnet.

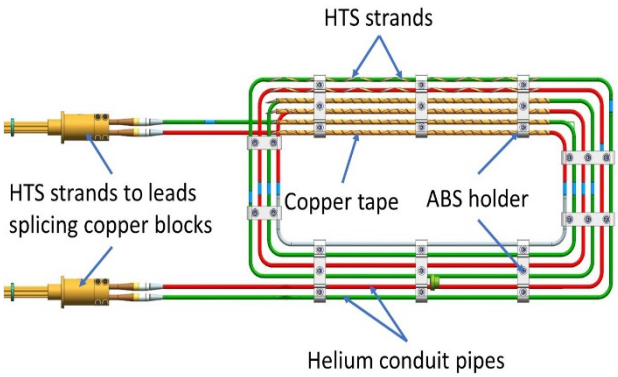

Figure 3: Design of 3-turn HTS magnet coil.

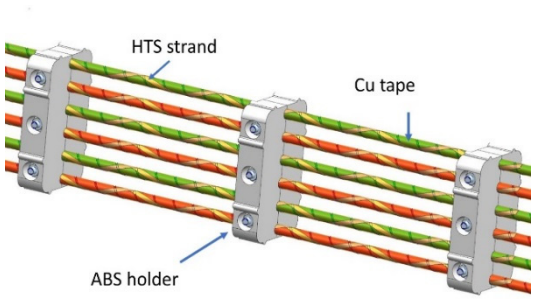

Figure 4: Expanded view of HTS magnet coil section.

Up to 12 HTS strands can be placed on each helium pipe but for the test magnet there are only 2 strands attached to each conduit pipe. There are 12 strands in the magnet power cable of 24 m total length of which 12 m is inside the magnet core. The electrical and magnetic properties of test magnet are given in Table 1. The projected critical current is 6 kA at 30 K. But lack of long-term stability of the supplied helium pressure has limited AC power supply operations to a maximum of I = 2 kA current to avoid the HTS conductor quench during the low helium pressure (~1 bar) and consequently high temperature (> 40 K) excursions.

The AC current source is constructed of three, 1.5 V switcher cells, similar to those reported in [9], arranged in series to maximize the output current while minimizing the required voltage.

Table 1: Properties of HTS Test Magnet

Parameter	value
Cable critical current @ 6.5 K	6 kA
Cable critical current @ 30 K	2 kA
Magnet critical current @ 30 K	6 kA
Magnet maximum applied current	1.9 kA
Magnet maximum B-field	0.23 T
Magnet resistance @ 6.5 K (leads @ RT)	340 Ω
Magnet resistance @ 6.5 K (cold leads)	150 Ω
Magnet inductance	96 µH
Leads inductance	4 µH

The test system arrangement is shown in Fig. 5, and the actual test setup in Fig. 6. The magnet HTS conductor coil and the conventional (copper) current leads are cooled using separate liquid helium flows. The pressure and temperature sensors are placed in the inlets and outlets of the helium cooling circuits. The liquid helium from the magnet coil and the current leads exits into the 3.6 kW pipe-type heaters which warm liquid helium to the room temperature before passing it into the flow meters and then returning under suction to the cryogenic plant. The difference in helium temperatures measured at the inlet and outlet of the conductor helium conduit pipe together with measured helium pressure and flow rate were used to determine the cryogenic power loss through the change of helium enthalpy which equals the change of system energy when combined with helium flow rate.

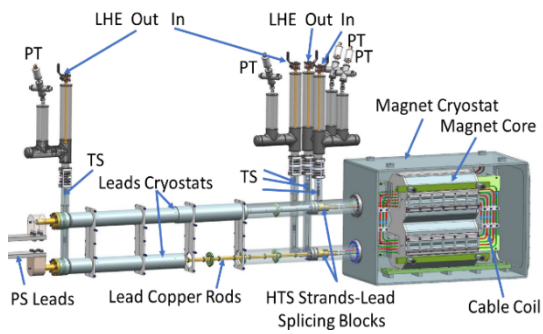

Figure 5: HTS magnet test arrangement.

Figure 6: HTS magnet test set-up.

ISBN: 978-3-95450-223-3 ISSN: 2673-7000 doi:10.18429/JACoW-NAPAC2019-WEPLH19

MAGNET POWER TEST RESULTS

As the result of the test, operating the AC power supply at the 20 Hz repetition rate with *dI/dt* = 38 kA/s current sine-wave, we obtained the *dB/dt* rate of 12 T/s in each of the magnet's two gaps – see Fig. 7. At such *B*-field cycling rate no measurable helium temperature rise in conductor loop was observed with temperature exposed sensors error of ±0.1 K. As presented in detail in [1] the combined analysis of cryogenic power loss measured in this test and the previous one [10] where the HTS strands were exposed to *dB/dt* of (4-20) T/s range indicates possibility that the cryogenic power loss for the test magnet could be as low as 0.06 W. Using this result we estimate required cryogenic power for the 8 GeV dual proton beam Booster accelerator operating with a current wave-form shown in Fig. 8.

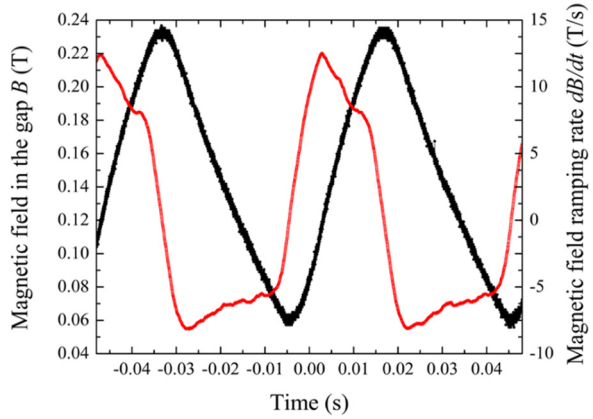

Figure 7: Magnetic field *B* (black line), left vertical axis and its ramping rate *dB/dt* (red line, right axis) at 20 Hz.

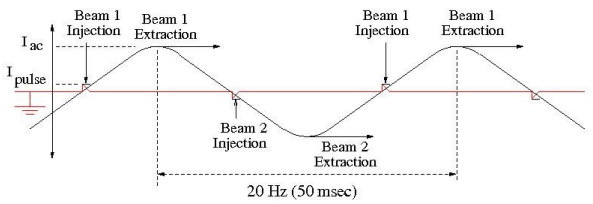

Figure 8: Current wave-form for acceleration of a dual proton beam. Small triangular pulses are imposed on the main current pulse to create flat tops facilitating injections.

Such a current wave-form allows for circulation of both proton beams in the same direction facilitating use of a common RF system. The selected parameters of 8 GeV dual proton beam Booster are given in Table 2.

The cost of Booster accelerator HTS strands (as used in the test magnet), would be about $ 4M, and the cost of the Fe3%Si laminations of the test magnet cross-section is about $ 25K/m, or $ 9 M for the 380 m long magnet string. The cost of 2 kW helium refrigerator at 4.5 K is $ 3M [11]. So, the cost of the HTS Booster basic components is about $ 16M. If the normal conducting magnets were used the magnet core cross-section area would have to significantly enlarge due more space required for the copper cable, and probably increasing just the cost of the laminations to the level of all HTS Booster basic components.

Table 2: Dual Proton Beam 8 GeV Booster Parameters

Component	Units	Value
Circumference	[m]	474
Magnet string length	[m]	380
Beam gaps (vert. x hor.)	[mm x mm]	50 x 100
B-field	[T]	+/- 0.7
Magnet current	[kA]	36
Repetition rate	[Hz]	20
dB/dt	[T/s]	36
Cryogenic power (proj.)	[kW]	1.9

We plan to improve the AC power and cryogenic systems to energize the HTS-based magnet prototype in the dB/dt range from 20 T/s to 200 T/s as required for the future muon accelerator [2], and expect to determine the AC power losses more accurately combining cryogenic and electrical measurement methods.

REFERENCES

[1] H. Piekarz, S. Hays, J. Blowers, B. Claypool and V. Shiltsev, "Record fast-cycling accelerator magnet based on HTS conductor," *Nucl. Instrum. Methods*, vol. 943, p. 162490, 2019. https://www.sciencedirect.com/science/article/pii/S016890021931037X?via%3Dihub

[2] D. Neuffer and V. Shiltsev, "On the feasibility of a pulsed 14 TeV c.m.e. muon collider in the LHC tunnel," *J. Instrum.*, vol. 13, p. T10003, 2018. https://doi.org/10.1088/1748-0221/13/10/T10003

[3] A. Milanese, L. Rossi, and H. Piekarz, "Concept of a Hybrid (Normal and Superconducting) Bending Magnet Based on Iron Magnetization for 80-100 km Lepton / Hadron Colliders", in *Proc. 5th Int. Particle Accelerator Conf. (IPAC'14)*, Dresden, Germany, Jun. 2014, pp. 980-982. doi:10.18429/JACoW-IPAC2014-TUOCB01

[4] M. Benedikt *et al.*, Report CERN-ACC-2018-0057, 2018.

[5] H. Piekarz, "Project X with Rapid Cycling and Dual Storage Superconducting Synchrotrons," arXiv:1205.1527, 2012.

[6] E. Prebys *et al.*, "Long Term Plans to Increase Fermilab's Proton Intensity to Meet the Needs of the Long Baseline Neutrino Program", in *Proc. 7th Int. Particle Accelerator Conf. (IPAC'16)*, Busan, Korea, May 2016, pp. 1010-1013. doi:10.18429/JACoW-IPAC2016-TUOAA03

[7] S. Nagaitsev and V. Lebedev, "A Cost-Effective Rapid-Cycling Synchrotron," arXiv:1812.10830, 2018.

[8] http://www.superpowerinc.com/system/files/SP_2G+Wire+Spec+Sheet_2014_web_v1.pdf

[9] S. Hays, B. Claypool, W. Foster, "The 100000 Amp DC Power Supply for a Staged Hadron Collider Superferric Magnet," *IEEE Trans. Appl. Superconductivity*, vol. 16, no. 2, p. 1626, 2006.

[10] H. Piekarz, S. Hays, J. Blowers, V. Shiltsev, "A Measurement of HTS Cable Power Loss in a Sweeping Magnetic Field," *IEEE Trans. Appl. Superconductivity*, vol. 22, no. 3, p. 5800105, 2012.

[11] M.A. Green, LBNL Report #63506, 2008.